Numerical analysis of unsteady flow and bed variation using temporal changes in water surface profiles during 1981 flood of the Ishikari river mouth

Seiji Okamura[1] and Shoji Fukuoka[2]

[1]Department of Science and Engineering,
Chuo University, Japan
E-mail: seijiokamura5@gmail.com
[2]Research and Development Initiative,
Chuo University, Japan
E-mail: sfuku@tamacc.chuo-u.ac.jp

Abstract

For the flood control and the river management, it is important to evaluate the degree of bed variation during floods. But accurate measurements of temporal changes in bed elevations during floods are difficult. In this study, we develop the quasi-3D unsteady flood flow and 2D bed variation analysis method using observed temporal changes in water surface profiles. This computational method utilizes the fact that the influences of channel shape, bed resistance and bed variation are reflected in temporal changes in water surface profiles. In the present method, the concentration of suspended sediment is calculated by 3D advection-diffusion equations. This paper shows that the present computation method can explain properly bed variation mechanism during the August 1981 flood of the Ishikari River which a large bed scouring at the river mouth occurred.

1. Introduction

For the flood control and the river management, it is important to evaluate the degree of bed variation during floods. But, it is difficult to elucidate temporal changes in bed elevations during the period of floods because of the difficulty of measurement.

Fukuoka et al. (2004) estimated the bed resistances and the discharge hydrographs by computing 2D unsteady flood flow so as to coincide with observed temporal changes in water surface profiles. This computational method is based on the idea that the influences of channel shape and resistance are reflected in temporal changes in water surface profiles. The influence of bed variation during flood is also reflected in temporal changes in water surface profiles where the large degree of bed variation occurs. For the purpose of river management, Fukuoka (2011) proposed an observation-calculation system of flood flow and sediment load focusing on temporal changes in water surface profiles to figure out flood flows and bed variations during floods. In the system, temporal changes in water surface profiles and discharge hydrographs during the period of floods and bed elevations before and after floods are observed at the sections in question. Then, we can figure out flood phenomena by computing the unsteady flood flow and bed variation so as to explain these observed data.

The objective of this study is to demonstrate that the bed variation mechanism during the August 1981 flood of the Ishikari River which a large bed scouring occurred in river mouth can be evaluated by the quasi-3D unsteady flow and 2D bed variation analysis using observed temporal changes in water surface profiles. In the analysis, the concentration of suspended sediment is calculated by 3D advection-diffusion equations in order to evaluate suspended load affected by the secondary flow in meandering channel.

2. The August 1981 Flood of the Ishikari River Mouth and the Previous Researches

2.1 Observation at the August 1981 Flood of the Ishikari River Mouth

Figure 1 shows observed discharge hydrograph of August 1981 flood of the Ishikari River mouth. The peak discharge of the flood exceeded the design discharge at that time and a large bed scouring occurred in the river mouth. During the flood, temporal data of water levels were measured at many observation points as shown in Figure 2. The cross-sectional bed forms were surveyed before and after the flood.

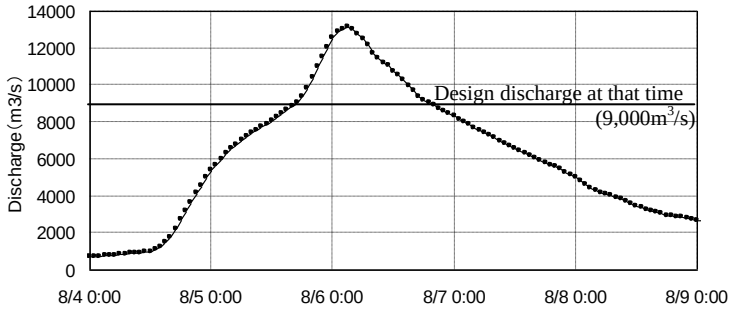

Figure 1: Discharge hydrograph of August 1981 flood of the Ishikari River mouth

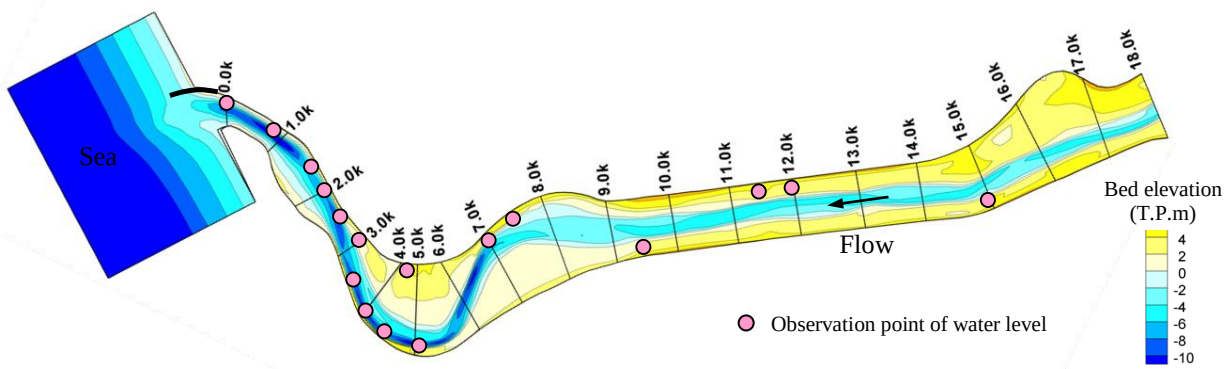

Figure 2: Plan-form and contour of bed level of the Ishikari River mouth and observation points of 1981 flood

2.2 Previous Researches

There have been a lot of researches on the bed variation of the flood. One of them, Shimizu et al. (1986) developed 1D quasi-steady flow and bed variation analysis considering the concentration of suspended sediment whose vertical distribution is assumed to be exponential curve. They indicated that suspended load is dominant for the bed variation in the Ishikari River mouth. Inoue et al. (2004) extended the above analysis to 2D quasi-steady flow and bed variation analysis considering the effect of secondary flow. Where, suspended load is calculated by concentration of suspended sediment and horizontal velocity whose vertical

distributions are assumed to be exponential and polynomial curves, respectively. But a problem to be solved remains that the bed scouring in meandering section was not explained well because the secondary flow due to meandering channel are not solved well by 2D flow analysis and because of the assumption of vertical distribution of suspended sediment concentration.

3. The Analysis of Bed Variation during 1981 flood in the Ishikari River Mouth

3.1 Computational Method

We develop a new method of the unsteady numerical analysis by solving 1981 flood flow and bed variation so as to coincide with observed temporal changes in water surface profiles. The discharge hydrograph and bed forms after the flood are compared with observed data. The validity of calculated temporal bed elevations during the flood are verified by temporal changes in observed water surface profiles. The analysis consists of quasi-3D unsteady flow analysis (Uchida and Fukuoka, 2009) as shown in Eq. (1) ~ (6) and 2D bed variation analysis for graded sediment (Fukuoka et al., 1998), employing the general coordinate system. The bed load is calculated by the formula of Fukuoka (2010).

In the quasi-3D unsteady flow analysis, the horizontal velocity u_i at $\zeta = (z_s - z)/h$ is assumed as shown in Eq. (1). Where $i,j = x,y$, δu_i = the difference between depth averaged velocity U_i and bottom velocity u_{bi}. δu_i is calculated by Eq. (2) using depth integrated vorticity Ω_i.

$$u_i - U_i = \frac{\delta u_i}{2}\left(1 - 3\zeta^2\right) \tag{1}$$

$$\delta u_i = U_i - u_{bi} = \frac{2}{3}\left(\varepsilon_{ij3}\Omega_j h - \frac{\partial Wh}{\partial x_i}\right) \approx \frac{2}{3}\varepsilon_{ij3}\Omega_j h \tag{2}$$

Where spatial change of depth averaged vertical velocity W is assumed to be negligible in shallow flows. Depth averaged horizontal velocity U is calculated by shallow water equations as shown in Eq. (3) ~ (5) employing the general coordinate system (ξ, η).

$$J\frac{\partial h}{\partial t} + \frac{\partial \Delta\eta U^{\xi} h}{\partial \xi} + \frac{\partial \Delta\xi U^{\eta} h}{\partial \eta} = 0 \tag{3}$$

$$\begin{aligned} &h\frac{\partial U^{\xi}}{\partial t} + U^{\xi}h\frac{\partial U^{\xi}}{\partial \tilde{\xi}} + U^{\eta}h\frac{\partial U^{\xi}}{\partial \tilde{\eta}} - \tilde{J}\left(U^{\eta} - U^{\xi}\cos\theta^{\eta\xi}\right)\left(U^{\xi}h\frac{\partial \theta^{\xi}}{\partial \tilde{\xi}} + U^{\eta}h\frac{\partial \theta^{\xi}}{\partial \tilde{\eta}}\right) = -gh\left(\frac{\partial z_s}{\partial \tilde{\xi}} + \cos\theta^{\eta\xi}\frac{\partial z_s}{\partial \tilde{\eta}}\right) \\ &-\tau_{0\xi} + \frac{1}{J}\left\{\frac{\partial}{\partial \xi}\left(\Delta\eta \cdot h\tilde{\tau}_{\xi\xi}\right) + \frac{\partial}{\partial \eta}\left(\Delta\xi \cdot h\tilde{\tau}_{\xi\eta}\right)\right\} - \tilde{J}h\left\{\left(-\tilde{\tau}_{\xi\xi}\cos\theta^{\eta\xi} + \tilde{\tau}_{\xi\eta}\right)\frac{\partial \theta^{\xi}}{\partial \tilde{\xi}} + \left(-\tilde{\tau}_{\xi\eta}\cos\theta^{\eta\xi} + \tilde{\tau}_{\eta\eta}\right)\frac{\partial \theta^{\xi}}{\partial \tilde{\eta}}\right\} \end{aligned} \tag{4}$$

$$\begin{aligned} &h\frac{\partial U^{\eta}}{\partial t} + U^{\xi}h\frac{\partial U^{\eta}}{\partial \tilde{\xi}} + U^{\eta}h\frac{\partial U^{\eta}}{\partial \tilde{\eta}} + \tilde{J}\left(U^{\xi} - U^{\eta}\cos\theta^{\eta\xi}\right)\left(U^{\xi}h\frac{\partial \theta^{\eta}}{\partial \tilde{\xi}} + U^{\eta}h\frac{\partial \theta^{\eta}}{\partial \tilde{\eta}}\right) = -gh\left(\cos\theta^{\eta\xi}\frac{\partial z_s}{\partial \tilde{\xi}} + \frac{\partial z_s}{\partial \tilde{\eta}}\right) \\ &-\tau_{0\eta} + \frac{1}{J}\left\{\frac{\partial}{\partial \xi}\left(\Delta\eta \cdot h\tilde{\tau}_{\eta\xi}\right) + \frac{\partial}{\partial \eta}\left(\Delta\xi \cdot h\tilde{\tau}_{\eta\eta}\right)\right\} - \tilde{J}h\left\{\left(-\tilde{\tau}_{\xi\xi} + \tilde{\tau}_{\xi\eta}\cos\theta^{\eta\xi}\right)\frac{\partial \theta^{\eta}}{\partial \tilde{\xi}} + \left(-\tilde{\tau}_{\xi\eta} + \tilde{\tau}_{\eta\eta}\cos\theta^{\eta\xi}\right)\frac{\partial \theta^{\eta}}{\partial \tilde{\eta}}\right\} \end{aligned} \tag{5}$$

Ω_i is calculated by horizontal vorticity equation as shown in Eq. (6).

$$\frac{\partial Jh\Omega_i}{\partial t} + \frac{\partial h\Delta\eta\left(F_{i\xi} + D_{i\xi}\right)}{\partial \xi} + \frac{\partial h\Delta\xi\left(F_{i\eta} + D_{i\eta}\right)}{\partial \eta} = J\left(ER_{zi} + P_{\omega i}\right) \tag{6}$$

Where $F_{i\xi}, F_{i\eta}$ = flux of Ω_i with expansion, contraction and rotation, $D_{i\xi}, D_{i\eta}$ = flux of Ω_i with diffusion, ER_{zi} = rotation term, $P_{\omega i}$ = production term.

3.2 Computational Method of Suspended Load

At the section in question, effects of suspended load are dominant for bed variation and vertical distributions of concentrations of suspended sediment are affected by the longitudinal deformation of channel shape and the secondary flow due to meandering channel. In this paper, we compare results of two different methods for calculating suspended sediment transport.

At first (as calculation case 1), the vertical distributions of concentration of suspended sediment is assumed as the exponential curves indicated by Lane-Kalinske (1950) as shown in Eq. (7). Vertical distributions of horizontal velocities are assumed as polynomial curves as shown in Eq. (8) in the quasi-3D unsteady flow analysis. Depth integrated fluxes of concentrations of suspended sediment are shown in Eq. (9).

$$c_k(z) = c_{bk} \exp\left(-\frac{w_{0k} z}{\varepsilon}\right) \tag{7}$$

$$u^i(z) = U^i - \frac{\delta u^i}{2}\left(\frac{3}{h^2} z^2 - \frac{6}{h} z + 2\right) \tag{8}$$

$$\overline{u^i c_k} = \frac{1}{h}\int_0^h \left(u^i c_k\right) dz = \frac{c_{bk}}{\beta}\left\{\left(\alpha\gamma^2 - U^i - \frac{\delta u^i}{2}\right)\exp(-\beta) - \left(\alpha\gamma(\gamma - h) - U^i + \delta u^i\right)\right\} \tag{9}$$

Where z = height from reference plane, $c_k(z)$ = concentration of suspended sediment of d_k(arbitrary grain diameter) at z, c_{bk} = reference concentration of suspended sediment of d_k, w_{0k} = falling velocity of grain, ε = coefficient of diffusion, $u^i(z)$ = horizontal velocity ($i = \xi, \eta$) at z, U^i = depth averaged velocity, $\delta u^i = U^i - u_b{}^i$, h = water depth, $\alpha = 3\delta u^i / h^2$, $\gamma = h/\beta = \varepsilon_s / w_{0k}$. Transport of suspended sediment concentration is calculated by horizontal 2D advection-diffusion equations as shown in Eq. (10).

$$\begin{aligned}&\frac{\partial C_k}{\partial t} + \frac{1}{J}\left(\frac{\partial \Delta\eta \cdot \overline{u^\xi c_k}}{\partial \xi} + \frac{\partial \Delta\xi \cdot \overline{u^\eta c_k}}{\partial \eta}\right) = \frac{\partial}{\partial \tilde{\xi}}\left(\varepsilon_s \cdot \frac{\partial C_k}{\partial \tilde{\xi}}\right) + \frac{\partial}{\partial \tilde{\eta}}\left(\varepsilon_s \cdot \frac{\partial C_k}{\partial \tilde{\eta}}\right) \\ &+ \cos\theta^{\eta\xi}\left\{\frac{\partial}{\partial \tilde{\xi}}\left(\varepsilon_s \cdot \frac{\partial C_k}{\partial \tilde{\eta}}\right) + \frac{\partial}{\partial \tilde{\eta}}\left(\varepsilon_s \cdot \frac{\partial C_k}{\partial \tilde{\xi}}\right)\right\} + \frac{\varepsilon_s}{\tilde{J}}\left\{\frac{\partial C_k}{\partial \tilde{\xi}}\frac{\partial \theta^\xi}{\partial \tilde{\eta}} + \frac{\partial C_k}{\partial \tilde{\eta}}\frac{\partial \theta^\eta}{\partial \tilde{\xi}}\right\} + q_{suk} - c_{bk} w_{0k}\end{aligned} \tag{10}$$

Where C_k = Depth averaged concentration of suspended sediment of d_k. Pick up rate of suspended sediment from bed surface (q_{suk}) is calculated by the formula of Itakura and Kishi (1980).

Next (as calculation case 2), in order to calculate the suspended load affected by the secondary flow directly, the concentration of suspended sediment is calculated by 3D advection-diffusion equations as shown in Eq. (11). Where, the velocities are calculated by quasi-3D unsteady flow analysis. This analysis can calculate vertical distribution of suspended sediment concentration due to secondary flow.

$$\frac{\partial c_k}{\partial t}+\frac{1}{J}\left(\frac{\partial \Delta\eta\cdot u^{\xi}c_k}{\partial \xi}+\frac{\partial \Delta\xi\cdot u^{\eta}c_k}{\partial \eta}\right)+\frac{\partial c_k\left(u^{\sigma}-\sigma_t-w_{0k}\right)}{\partial \sigma}=\frac{\partial}{\partial \tilde{\xi}}\left(\varepsilon_s\cdot\frac{\partial c_k}{\partial \tilde{\xi}}\right)+\frac{\partial}{\partial \tilde{\eta}}\left(\varepsilon_s\cdot\frac{\partial c_k}{\partial \tilde{\eta}}\right) \tag{11}$$
$$+\cos\theta^{\eta\xi}\left\{\frac{\partial}{\partial \tilde{\xi}}\left(\varepsilon_s\cdot\frac{\partial c_k}{\partial \tilde{\eta}}\right)+\frac{\partial}{\partial \tilde{\eta}}\left(\varepsilon_s\cdot\frac{\partial c_k}{\partial \tilde{\xi}}\right)\right\}+\frac{\varepsilon_s}{\tilde{J}}\left\{\frac{\partial c_k}{\partial \tilde{\xi}}\frac{\partial \theta^{\xi}}{\partial \tilde{\eta}}+\frac{\partial c_k}{\partial \tilde{\eta}}\frac{\partial \theta^{\eta}}{\partial \tilde{\xi}}\right\}+\frac{\partial}{\partial z}\left(\varepsilon_s\cdot\frac{\partial c_k}{\partial z}\right)+q_{suk}$$

3.3 Computational Conditions

The initial bed forms before 1981 flood were surveyed in 1979 and shown in Figure 2. The boundary conditions of upstream and downstream ends are given by observed water level hydrograph at 15km point and tide levels of the Otaru tidal observatory near the river mouth, respectively. The mean grain diameter is 0.3mm downstream of 8km and 0.8mm upstream of 8km. The Manning's roughness coefficients are determined so as to minimize the difference between temporal changes in the observed and the calculated water surface profiles. As a result, n=0.013 for the main channel downstream of 8km, n=0.021 for the main channel upstream of 8km and n=0.050 for flood plains are given.

3.4 Computational Results

Figure 3 shows temporal changes in observed and calculated water surface profiles in flood rising and falling periods. Calculated water surface profiles coincide with observed water levels affected by bed variations in each time and there are little differences between calculated water levels of each calculation cases. Figure 4 shows the comparison between observed and calculated longitudinal bed forms before and after the flood. In the Ishikari River mouth, suspended load causes the bed variations. The width-averaged bed elevations after the flood of each calculation cases are similar and nearly coincide with that of observed result. On the other hand, clear differences between each calculation cases can be seen in the lowest bed elevations of the meandering section from 3km to 8km.

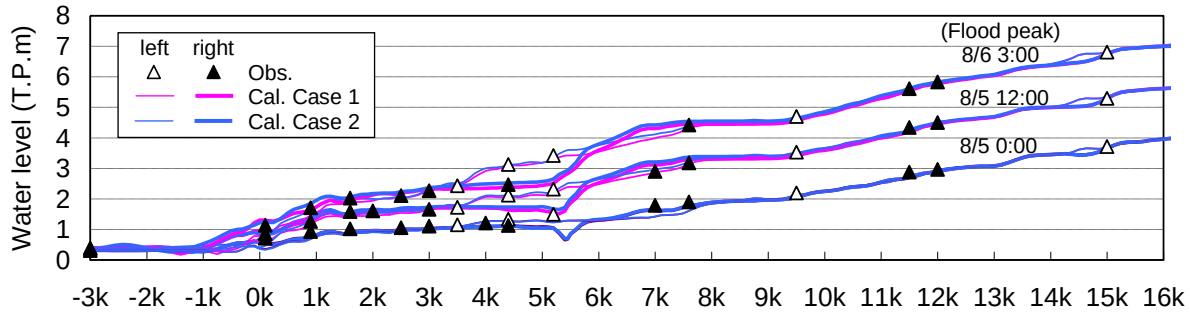

(a) Flood rising period

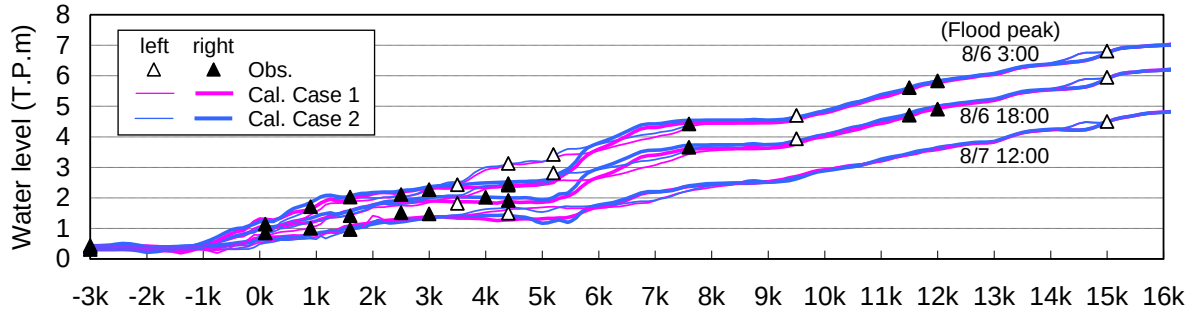

(b) Flood falling period

Figure 3: Temporal changes in observed and calculated water surface profiles

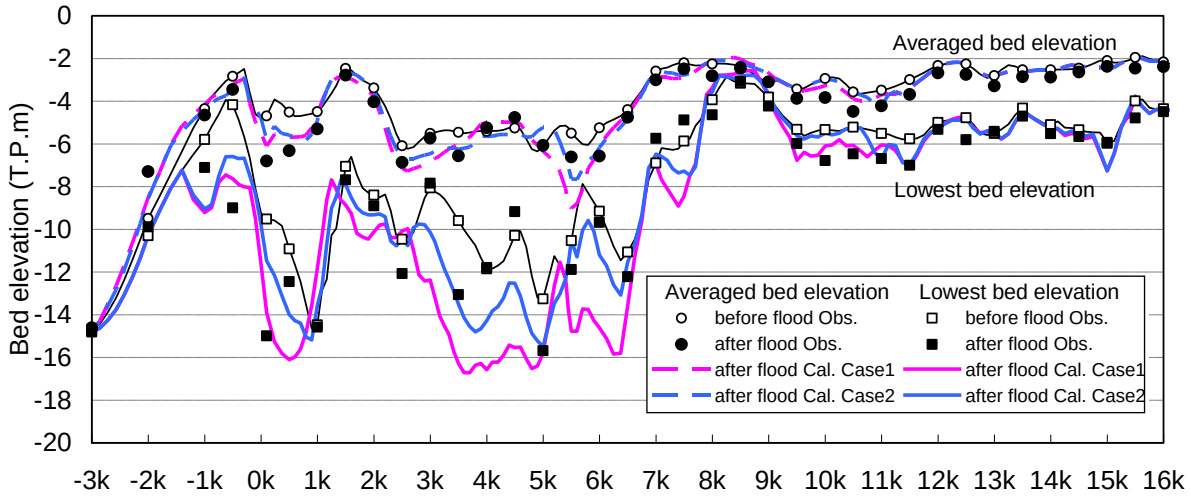

Figure 4: Average and lowest bed elevations before and after 1981 flood

Figure 5 shows cross-sectional bed forms of observation and calculations in meandering section from 3.5km to 6.5km before and after the flood. The bed scourings are observed near the left banks at 3.5km and 4.0km. On the other hand, the observed cross-sectional bed slopes are almost flat at 5.5km and 6.0km. The cross-sectional bed slopes of calculation case 1 (using Eq. (10)) are steeper than those of the observation at 3.5km and 4.0km and the scourings occur near right banks at 5.5km and 6.0km. On the other hand, the cross-sectional bed slopes of calculation case 2 (using Eq. (11)) nearly coincide with those of the observation.

Figure 6 shows vertical distributions of calculated lateral velocities and concentrations of suspended sediment at 5.5km cross-section in flood rising period. The secondary flows due to meandering channel can be seen at 5.5km cross-section as shown in Figure 6(a). The flows near the bed transport suspended sediment near the bed. Therefore, there are small concentrations at left bank and large at right bank in calculation case 2 (the concentrations of suspended sediment are calculated by 3D advection-diffusion equations) as shown in Figure 6(b).

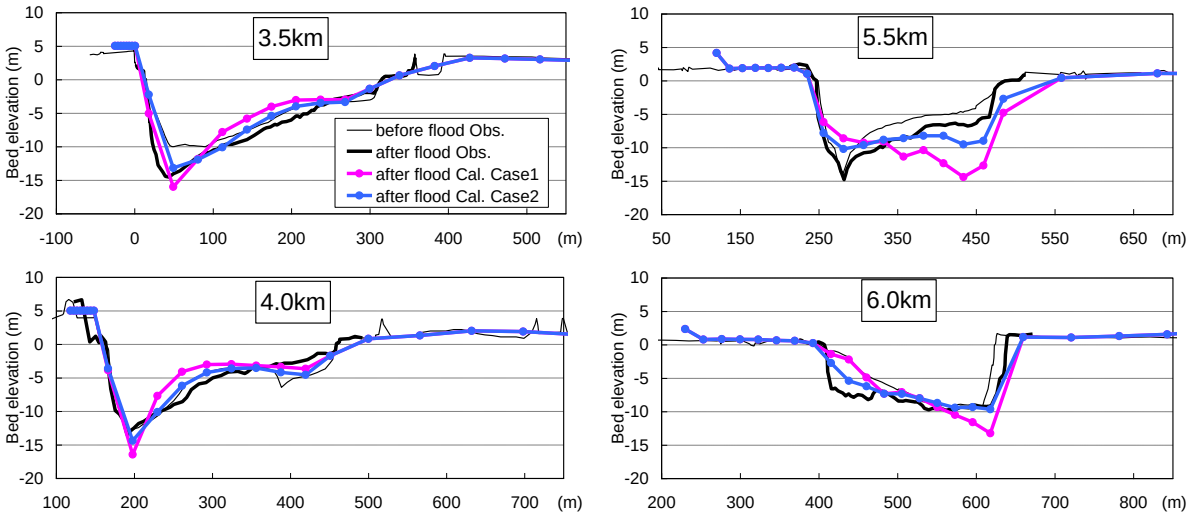

Figure 5: Cross-sectional bed forms from 3.5km to 6.0km cross section before and after 1981 flood

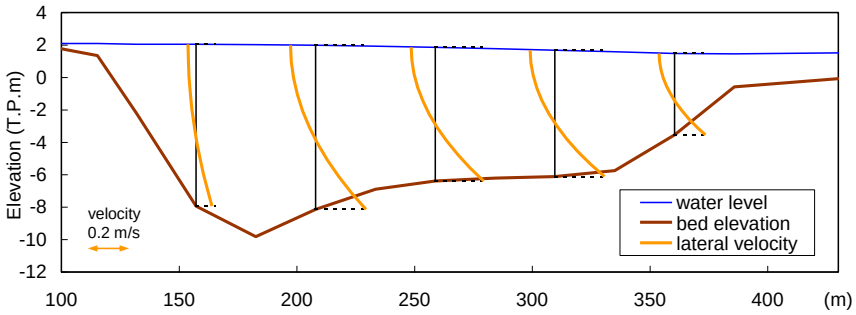

(a) Vertical distributions of calculated lateral velocities

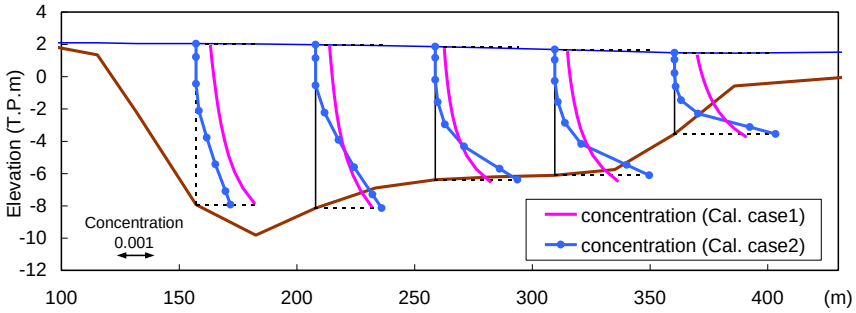

(b) Vertical distributions of calculated concentrations of suspended sediment

Figure 6: Vertical distributions of calculated lateral velocities and concentrations of suspended sediment at 5.5km cross-section in flood rising period

The discharge hydrograph is calculated by using temporal change of water surface profiles as shown in Figure 7. The accuracy of the observed discharge is not so high because large temporal changes in bed elevations are not considered. Calculated discharge hydrograph seems to be reliable more than observed one.

As above, the analysis evaluates properly the flood flow and the bed variation during 1981 flood of the Ishikari River mouth.

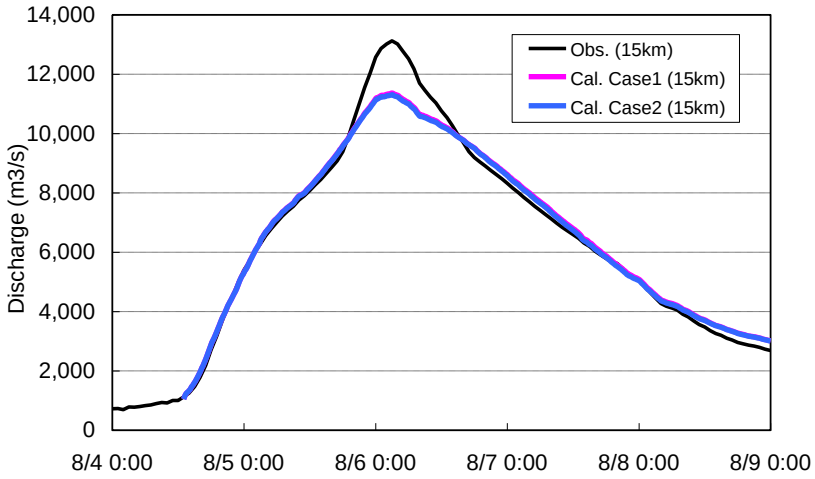

Figure 7: Discharge hydrograph at 15km upstream from the river mouth

4. Conclusions

In this paper, we develop the computation method of the quasi-3D unsteady flow and 2D bed variation and calculate the August 1981 flood of the Ishikari River using observed temporal changes in water surface profiles.

The bed variation mechanism during the 1981 flood can be evaluated by the present analysis which explains well the discharge hydrograph during the flood period and bed elevations surveyed after the flood.

Longitudinal changes in the cross-sectional bed forms at meandering section are calculated appropriately by the present analysis. The main reason is because the suspended load transported by the secondary flow in the meandering section is solved well by the analysis of the quasi-3D unsteady flow and the 3D advection-diffusion equations of suspended sediment concentration.

References

Fukuoka, S., Watanabe, A. and Okada, S. (1998) Bed topography analysis in a compound meandering channel by using 3D numerical model with approximation of hydrostatics pressure. *Annual Journal of Hydraulic Engineering,* Vol.42, 1015-1020, JSCE.

Fukuoka, S. (2010) River engineering adaptations against the global warming – Towards generalization of close-to-nature rivers. *Proceedings of the Japan Society of Civil Engineers,* F, Vol.66, No.4, 471-489, JSCE.

Fukuoka, S. (2011) What is the fundamentals of river design – Utilization of visible techniques of sediment laden-flood flows. *Advances in River Engineering,* Vol.17, 83-88, JSCE.

Inoue, T., Hamaki, M., Arai, N., Nakata, M., Takahashi, T., Hayashida, K., and Watanabe, Y. (2004) Quasi-three-dimensional calculation of riverbed deformation during 1981-year flood in the Ishikari River mouth. *Advances in River Engineering,* Vol.10, 101-106, JSCE.

Itakura, T. and Kishi, T. (1980) Open channel flow with suspended sediments. *Journal of Hydraulics Division, Proceedings of ASCE,* Vol.106, HY.8, 1325-1343.

Shimizu, Y., Itakura, T., Kishi, T. and Kuroki, M. (1986) Bed variations during the 1981 August flood in the lower Ishikari River. *Annual Journal of Hydraulic Engineering,* Vol.30, 487-492, JSCE.

Takagi, J., Makino, N., Takemoto, N. and Morita, Y. (1982) Field survey of flood flow and bed evolution in the lower Ishikari River. *Annual Journal of Hydraulic Engineering,* Vol.26, 57-62, JSCE.

Uchida, T. and Fukuoka, S. (2009) A depth integrated model for 3D turbulence flows using shallow water equations and horizontal vorticity equations. *33rd IAHR Congress, Water Engineering for a Sustainable Environment,* 1428-1435.